Psychophysiology, 46 (2009), 344–356. Wiley Periodicals, Inc. Printed in the USA.
Copyright © 2009 Society for Psychophysiological Research
DOI: 10.1111/j.1469-8986.2008.00777.x

Phenotypic and genetic correlations between evoked EEG/ERP measures during the response anticipation period of a delayed response task

DIRK J. A. SMIT,[a] DANIELLE POSTHUMA,[a,b] DORRET I. BOOMSMA,[a] AND ECO J. C. DE GEUS,[a,b]

[a]Biological Psychology, Cognitive Research, VU University Amsterdam, 1081 BT Amsterdam, the Netherlands
[b]Centre for Neurogenomics and Cognitive Research, VU University Amsterdam, 1081 HV Amsterdam, the Netherlands

Abstract

We investigated the relationship between three electrophysiological indices of response anticipation in a spatial delayed response task with a low and high memory load manipulation: a slow cortical potential (SCP), theta desynchronization, and upper alpha synchronization. Individual differences in these three measures were examined in 531 adult twins and siblings. Heritability of the SCP at occipital-parietal leads varied from 30% to 43%. Heritability of upper alpha synchronization (35% to 65%) and theta desynchronization (31% to 50%) was significant at all leads. Theta desynchronization and upper alpha synchronization were significantly correlated ($r \sim 43\%$), but SCP was not correlated with either. The effect of working memory load on all three measures was not heritable. Response anticipation reliably evokes an SCP, upper alpha synchronization and theta desynchronization, but variation in these measures reflects different (genetic) sources.

Descriptors: Alpha oscillations, Theta oscillations, Slow cortical potentials, Individual differences, Endophenotype

A warning stimulus preceding a later imperative stimulus generates a Slow Cortical Potential (SCP; Altenmüller & Gerlof, 1999; Fan et al., 2007; Rockstroh, Elbert, Canavan, Lutzenberger, & Birbaumer, 1989; Walter, Cooper, Aldridge, McCallum, & Winter, 1964). Two well-known examples of SCPs are the *Bereitschaftspotenzial* (readiness potential), a negative DC shift seen in anticipation of a voluntary movement, and the contingent negative variation, a negative shift in the interval between a warning tone and a response initiating imperative stimulus with predictable timing (Altenmüller & Gerloff, 1999; Rockstroh et al., 1989; Walter, 1964).

SCPs can be elicited in spatial and nonspatial delayed response tasks (Birbaumer, Elbert, Canavan, & Rockstroh, 1990; Hansell et al., 2001). In these tasks, a target stimulus acts as the warning stimulus, and a second stimulus event controls timing of the response, which results in a slow negative event-related potential (ERP) wave with a frontocentral maximum. Working memory load in the interstimulus interval strongly enhances the magnitude of the SCP (Ruchkin, Canoune, Johnson, & Ritter, 1995), as do motivational aspects, including positive (reward level) and negative (shock avoidance) motivators (Birbaumer et al., 1990).

Delayed response tasks of the type that evoke an SCP have also been reported to produce a small but consistent upper alpha synchronization (Bastiaansen, Posthuma, Groot, & de Geus, 2002; Jensen, Gelfand, Kounios, & Lisman, 2002; Klimesch, Doppelmayr, Schwaiger, Auinger, & Winkler, 1999; Sauseng, Klimesch, Schabus, & Doppelmayr, 2005). It seems plausible to hypothesize that electroencephalographic (EEG) phenomena sharing antecedent conditions may also share neural substrates. The thalamo-cortical connections may be such a substrate for the SCP and alpha oscillatory activity. Thalamic activity has been shown to be correlated to the SCP (Birbaumer et al., 1990; Strehl et al., 2006), and thalamo-cortical connections are essential in the formation of alpha oscillatory activity (Steriade, 2000). In addition, the SCP has been shown to correlate on a trial-by-trial basis with fMRI BOLD signal in the thalamus (Nagai et al., 2004), and lateral thalamic metabolic rate has also been found to correlate highly with alpha power (Danos, Guich, Abel, & Buchsbaum, 2001; Goldman, Stern, Engel, & Cohen, 2002; Schreckenberger et al., 2004). The SCP and alpha synchronization may even be flip sides of the same coin, as it has been argued that ERPs (partially) arise from changes in ongoing oscillatory activity through phase locking (Klimesch, Sauseng, & Hanslmayr, 2007; Min et al., 2007; Sauseng et al., 2005) or through desynchronization of oscillations with a nonzero mean (Nikulin et al., 2007).

This research was funded by grants from the Human Frontiers of Science program RG0154/1998-B and the Netherlands Science Organization NWO/SPI 56-464-14192.

Address reprint requests to: Dirk Smit, Biological Psychology, Cognitive Research, VU University Amsterdam, van der Boechorststraat 1, 1081 BT Amsterdam, the Netherlands. E-mail: dja.smit@psy.vu.nl

Apart from the SCP and alpha synchronization, delayed response tasks have also been shown to generate theta desynchronization during the interval between the warning and imperative stimulus (Bastiaansen et al., 2002). As with the SCP, this theta synchronization showed sensitivity to increases in working memory load. Currently, a possible joint neural substrate for SCP and theta synchronization is less clear than one between the SCP and alpha synchronization. Changes in theta activity are related to changes in activity in cortico-hippocampal loops (Bastiaansen & Hagoort, 2003), but no studies have linked such loops to the SCP. By virtue of sharing the same antecedent conditions, however, theta desynchronization may be hypothesized to partly reflect the same neural substrate as the SCP and alpha synchronization.

Large individual differences are apparent for SCP, upper alpha synchronization, and theta synchronization, and various studies have linked these differences to variation in cognitive ablities (e.g., Basile et al., 2007; Doppelmayr, Klimesch, Hödelmoser, Sauseng, & Gruber, 2005; Doppelmayr, Klimesch, Sauseng, et al., 2005; Hansell et al., 2005; Jausovec & Jausovec, 2004; Klimesch, 1999; Perez-Edgar, Fox, Cohn, & Kovacs, 2006). If these ERP/EEG measures are indeed based on the same neural substrate, we expect that individual differences in SCP, upper alpha synchronization, and theta desynchronization are correlated. Furthermore, we expect that the change in these measures as a result of an increased working memory load or a motivational manipulation also shows a cross-measure correlation, such that individuals that show large (or small) increases in SCP amplitude as a function of experimental task load also show large (or small) changes in alpha synchronization and theta desynchronization. The current study aimed to test these expectations.

First, we tested whether interindividual variation in the three ERP/EEG measures during response anticipation was correlated, which would be predicted if they share a neural substrate. Second, because variation in EEG/ERP measures tends to be under strong genetic control (e.g., Smit, Posthuma, Boomsma, & de Geus, 2005; Smit, Posthuma, Boomsma, & de Geus, 2007a; Smit, Stam, Posthuma, Boomsma, & de Geus, 2008; van Beijsterveldt & van Baal, 2002), we tested whether heritability of the three ERP/EEG measures could be explained by a common genetic factor. Third, in keeping with the idea that challenges to the system tend to increase genetic variance (de Geus, Kupper, Boomsma, & Snieder, 2007), heritability of the ERP/EEG measures were examined under two levels of task difficulty: a low and a high memory load condition. We tested whether the increased memory load led to an increase in genetic variance and/or reduced error variance in all three measures. Finally, we tested whether the increase in genetic variance was due to newly emerging genetic effects specific to the high memory load condition.

Methods

Participants

The EEG sample in this study was derived from an ongoing twin family study on cognition (e.g., Posthuma, Neale, Boomsma, & de Geus, 2001; Smit et al., 2005, 2008; Smit, Posthuma, Boomsma, & de Geus, 2007a, 2007b) in twins and family members from the Netherlands Twin Registry (Boomsma, Vink, et al., 2002). It consisted of 760 subjects from 309 families divided into two age cohorts based on the age of the twins: a younger cohort ($M = 26.2$ years, $SD = 4.1$) and a middle-aged cohort ($M = 49.4$ years, $SD = 7.2$). On average, 2.50 participants per family participated; family size ranged from one to seven siblings (including twins). Informed consent was obtained in writing. The study received approval from the VU university ethical committee.

Apparatus

Subjects were seated in a comfortable reclining chair in a dimly lit, sound-attenuated, and electromagnetically shielded room. A touch-sensitive computer screen was placed 80 cm in front of the subjects. The chair was adjusted such that the center of the screen was at eye level. Subjects read the task instructions from a written sheet. For responding, subjects used a rubber tipped pointer (5 mm diameter) to touch the screen. The pointer was held like a pen, in the preferred hand. Before the trial started, subjects placed their hand on a 5×5 cm^2 response pad placed centrally in front of them, 20 cm in front of the screen. Release of the response pad was used to indicate the end of response initiation time and the start of the movement time. Screen touch with the pen constituted the end of the movement time.

The screen background was dark gray. A black hood with a 205-mm diameter hole in the middle was fastened to the monitor face to ensure that stimuli at all locations were at an equal distance from the edge of the screen.

Delayed Response Task

In Figure 1, the time course of a single trial in the delayed response task is schematically depicted. Each trial started with an auditory beep (100 ms at 1000 Hz) followed at offset by the appearance of a black fixation square (width about 0.5 cm, visual angle 0.36°) in the center of the screen. At 250 ms after onset of the fixation square, the target, a checkered black circle (diameter about 1.5 cm, visual angle 1.07°) was presented anywhere on an annulus (9.25 cm, 6.60°) from the fixation square, except for four symmetrical areas around the vertical and horizontal meridians. At the imperative stimulus, the offset of the central fixation square, the subject had to lift his or her hand from the response pad and touch the screen as accurately and as quickly as possible. In the low memory load condition, the target remained visible until the onset of the imperative stimulus. In the high memory load condition, the target disappeared 150 ms after onset, so that the subjects had to memorize the location of the target until the onset of the imperative stimulus. Two types of delay intervals were used, in which the fixation square either disappeared 1150 ms after target onset (short delay) or 4150 ms after target onset (long delay).

Before the actual task was started, subjects engaged in a 10-min training session (data not used). The actual task consisted of a total of 240 trials split into two 120-trial blocks lasting about 14 min each. In 224 trials, targets were presented in either the left or right, top and bottom visual fields at 7.58° off the vertical and horizontal meridians. There were 16 trials in which the target was presented within the meridian areas. These "catch trials" were included to increase the average spatial effort required, but were not used in the analyses. There were 96 trials in the low memory load condition and 132 trials in the high memory load condition. Half of each had a long delay interval (48 and 66 trials, respectively), the other half a short delay interval. Additionally, in half of the trials, a distractor was presented in a random position in the annulus but not within a 1.58° radius of the target position, which was identical to the target in shape and size.

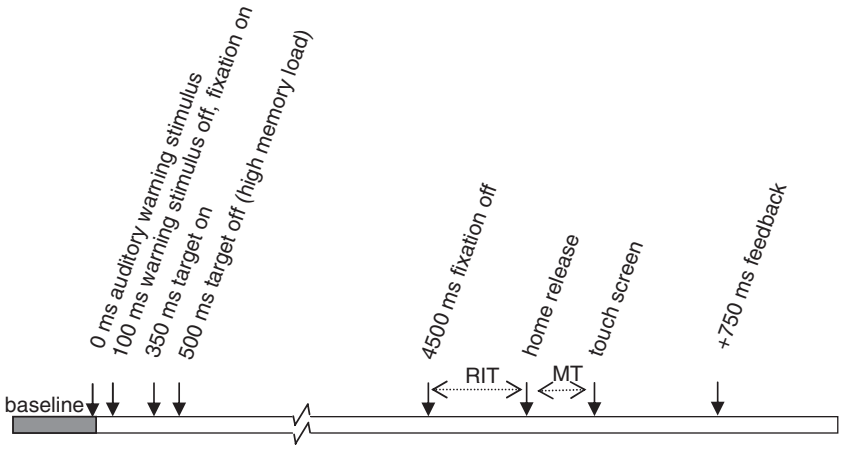

Figure 1. Timeline of a single trial. For a description of the stimuli see text. The trial begins with an auditory warning tone. The delay interval is defined from target offset (500 ms) to fixation offset (imperative stimulus; 4500 ms) for high memory load trials. Low memory load trials did not have a target offset and acted as the control condition. Response initiation time (RIT) and movement time (MT) were both variable. Feedback was presented a fixed 750 ms after touching of the screen or after the response deadline.

Distracters lasted 150 ms with an onset of 300–700 ms after target onset.

The order of presentation of the total set of the 240 possible trials was randomized once and was the same for each subject. For a trial to be correct at the behavioral level, the response initiation time needed to fall within an interval of 0.1 and 1.5 s after fixation offset (the imperative stimulus), and the screen had to be touched within 1.5 and 3 s after fixation offset within a radius of 2 cm of the target center. Spatial accuracy of correct trials was further quantified to determine the points earned by the subjects: touching within the center target area (0.4 cm) earned 10 points, off target responses earned 8 (0.4–0.8 cm), 6 (0.8–1.2 cm), 4 (1.2–1.6 cm), or 2 (1.6–2 cm) points. Feedback was displayed 250 ms after touching the screen, in the center of the screen, for a period of 1500 ms. This included a running total of the winnings so far and the number of points won or lost at the preceding trial. Touching outside of the target area lost 5 points and a red error message INCORRECT was displayed. Lifting the hand before offset of the fixation spot caused TOO FAST to be displayed. If the maximal response initiation time of 1500 ms expired, TOO SLOW was signaled. After feedback offset, a variable intertrial interval of 250 to 750 ms was followed by onset of the next trial.

Behavioral accuracy was indexed with the number of points earned in the task as described above. However, all incorrect trials received a score of 0 instead of the 5 indicated as feedback on the screen. Therefore, behavioral scores ranged from 0 to 10. Behavioral speed was computed across correct trials only and indexed by the interval between fixation offset and the moment of the release of the home button indicating the response initiation time.

EEG Recording

EEG was recorded for 3 min with 19 Ag/AgCl electrodes mounted in an electrocap. Earlobe reference electrodes A1 and A2 were measured unlinked for later digital recalculation of the reference. The ground electrode was attached to the forehead. Signal registration was conducted using an amplifier developed by Twente Medical Systems (TMS; Enschede, The Netherlands) for 657 subjects (381 young, 380 middle-aged) and NeuroScan SynAmps 5083 amplifier for 103 subjects (24 young, 80 middle-aged). Signals were continuously represented online on a Nec multisync 17-in. computer screen using Poly 5.0 software or Neuroscan Acquire 4.2. Standard 10–20 positions were F7, F3, F1, Fz, F2, F4, F8, T7, C3, Cz, C4, T8, P7, P3, Pz, P4, P8, O1, and O2. The vertical electro-oculogram (EOG) was recorded in bipolar derivation between two Ag/AgCl electrodes, affixed 1 cm below the right eye and 1 cm above the eyebrow of the right eye. The horizontal EOG was recorded bipolarly between two Ag/AgCl electrodes affixed 1 cm left from the left eye and 1 cm right from the right eye. An Ag/AgCl electrode placed on the forehead was used as a ground electrode. Impedances of all EEG electrodes were kept below 3 kΩ, and impedances of the EOG electrodes were kept below 10 kΩ. The EEG was amplified, digitized at 250 Hz, and stored for off-line processing. Amplifier filter settings for TMS were a single order FIR bandpass filter with cutoff frequencies of 0.05 Hz and 30.0 Hz. NeuroScan filter settings were a lowpass filter at 50.0 Hz.

EEG Data Processing

The signals were recalculated with averaged earlobes (A1 and A2) as reference. All EEG was automatically and visually checked for bad channels such as absence of signal, hum, clipping, persistent muscle tone artifacts, and external noise. Files were epoched with a 0.5-s baseline before the warning stimulus to 7.5 s after the warning stimulus. For each subject, artifactual epochs were identified automatically using the EEGLAB (Delorme & Makeig, 2004) ''reject by threshold'' and ''reject by spectra'' options. Threshold settings for all leads was $\pm$ 200 μV. The spectral analysis procedure identified deviant epochs by comparing each epoch's power spectrum to the spectrum averaged over all epochs. Epochs with more than 32 dB excess power within the frequency range below alpha (1.0–8.0 Hz) or above alpha (13.0–30.0 Hz) were marked artifacts. Visual inspection confirmed these epochs and corrections were made as necessary. If less than 29 trials were available for either condition due to either behavioral errors or EEG artifacts, the particular lead was marked as missing for this subject.

Next, EEGLAB was used to identify eye movement and blink sources of activation using Independent Components Analysis (ICA) decomposition based on the infomax algorithm (Makeig, Jung, Bell, Ghahremani, & Sejnowski, 1997). After ICA analysis

on both EEG and EOG data, components were identified that were related to artifactual sources and were removed (Delorme & Makeig, 2004). Eye movement and blink artifacts can be identified by frontal scalp distribution (lateralized for horizontal eye movements), high correlation with EOG signals, and a match in timing for clear blinks and/or saccades. A large proportion (97%) of the subjects revealed a first vertical EOG-related component, and 91% a second, horizontal EOG related component as independent component number 2. A small subset (13%) revealed a third component that seemed to reflect separate aspects of EOG movement and/or blink activity.

ERPs and EEG frequency measures were derived by averaging across all correct trials. Only the trials with a long delay interval (48 low and 66 high memory load trials) will be considered in this article, because previous analyses have shown that the upper alpha synchronization appears shortly after the stimulus-locked perturbations due to the stimulus events, and will not have fully appeared in the short delay interval (Bastiaansen et al., 2002). Because EEG/ERP data were not sufficiently different in distractor and nondistractor trials, these two trial types were collapsed to increase the total number of trials in the low and high memory load conditions. The removal of artifactual epochs and incorrect trials resulted in an average of 45.5 and 58.6 trials available for the low and high memory load conditions, respectively.

The SCP was scored as the average potential in the interval of 1800 to 4500 ms after warning stimulus onset. Time-frequency analysis used the event-related spectral perturbation algorithm *timef* as implemented in EEGLAB (Delorme & Makeig, 2004; Makeig, 1993). Power was estimated from 1.95 Hz to 49.8 Hz in 50 linearly spaced frequencies 0.98 Hz apart. Sine and cosine wavelets with a Hanning envelope—resulting in wavelets highly similar to Gaussian windowed Morlet wavelets—were used to estimate power in the 0.5-s baseline period and the 7-s period after warning stimulus onset. Wavelets were maximally 256 sample wide (1024 ms) at the lowest 1.95 Hz frequency, containing precisely 2 cycles of the sine and cosine. This window size was decreased to 128 samples width at the maximum frequency, thus enveloping 27 cycles of the 49.8-Hz sine and cosine. The number of cycles enveloped by the wavelet windows at in-between frequencies was linearly increased from 2 to 27. All wavelets were applied at 200 linearly spaced time points windows from 12 ms to 6988 ms after the warning stimulus onset. Baseline power was calculated using similar Hanning tapered wavelets 128 samples wide (512 ms) holding sines and cosines of the same 50 frequencies. This included a single cycle of the lowest frequency (1.95 Hz) and 25 cycles of the highest frequency (49.8 Hz). These wavelets were applied to the baseline extending slightly after auditory warning tone (500 to 12 ms). All power values were calculated as the squared absolute values of the complex numbers that were the result of the wavelet application to the data. Subsequently, all scores were log-transformed using the following formula:

$$\text{dB power} = 10 \cdot \log 10(power),$$

in units of $\log(\mu V^2)$. Next, log-transformed baseline power was subtracted from the poststimulus log-power values.

Theta desynchronization was scored in the same interval as the SCP of 1800 to 4500 ms after warning stimulus onset by averaging all data points in frequency bins 4.9 and 5.9 Hz. Upper alpha synchronization was scored by averaging all data points in frequency bins 9.8 and 10.8 Hz in the same interval.

Genetic Analyses

We first established the heritability of SCP, upper alpha synchronization, and theta desynchronization using the extended twin design (Posthuma et al., 2003). This design uses information on the genetic relatedness and on the sharing of environmental influences between twins and siblings to model resemblance on a (psychophysiological) trait (Boomsma, Bushjan, & Peltonen, 2002). Genetic relatedness varies between twins and siblings: monozygotic (MZ) twins share 100% of their genetic makeup, whereas dizygotic (DZ) twins and siblings share on average 50% of their segregating genes. If the correlation of psychophysiological scores between DZ twins or siblings is half the correlation between MZ twins, this is seen as evidence for additive genetic influences (A) on SCP variation. If the correlation between DZ twins or siblings is less than half the correlation between MZ twins, this is seen as evidence for dominant (nonadditive) genetic influences (D) on the total variation of a trait. If the correlations between MZ and DZ twins/siblings are comparable and nonzero, this is evidence for common environmental influences (C). If the correlation between MZ twins is not unity, this is evidence for environmental effects that are unique to each individual (E), which includes measurement error.

By using structural equation modeling, maximum likelihood estimates were obtained of the relative contributions of each of these unobserved factors (A, D or C, and E) to the total variance in the SCP, upper alpha synchronization, and theta synchronization. Because in the extended twin design there is not enough information available to estimate the effects of both C and D simultaneously, we used a model with A, D, and E if the DZ/sibling correlation was less than half the MZ correlation and a model with A, C, and E if it was more than half the MZ correlation. Heritability of the ERP/EEG measures was defined under the best fitting model as the additive (and, if applicable, dominant) genetic effects divided by the total variance. Figure 2 shows a univariate path model that represents the genetic model for two family members.

Second, we estimated the phenotypic (r_P) correlations between all possible pairs of SCP, upper alpha synchronization, and theta synchronization. We decomposed these as follows:

$$r_P = a_1 r_A a_2 + c_1 r_C c_2 + e_1 r_E e_2,$$

where r_A, r_C, and r_E denote the correlations between the additive genetic, common environmental, and unique environmental factors for each pair of measures. These factor correlations are weighted by the path loadings of both measures. In other words, the phenotypic correlation is a summation of the weighted genetic and environmental correlations. When the alternative model is fitted that excludes C and includes D, $c_1 r_C c_2$ must be substituted with $d_1 r_D d_2$.

Finally, we modeled the effects induced by the manipulation of memory load on SCP, upper alpha synchronization, and theta synchronization. We used a bivariate genetic model, as shown in Figure 3, to estimate the genetic contribution in the low and high memory load conditions simultaneously (see de Geus et al., 2007). In this case, the first genetic factor A1 is shared between both memory load conditions, whereas genetic factor A2 represents the effect of genes specific to the high memory load condition. Therefore, this second factor represents novel genetic influences that emerge with an increase in working memory load. Significance of this emergence is tested by comparing the fit of a model with factors A1 and A2 to a model that only models genetic factor A1. Note that if the path from A2 to the phenotype

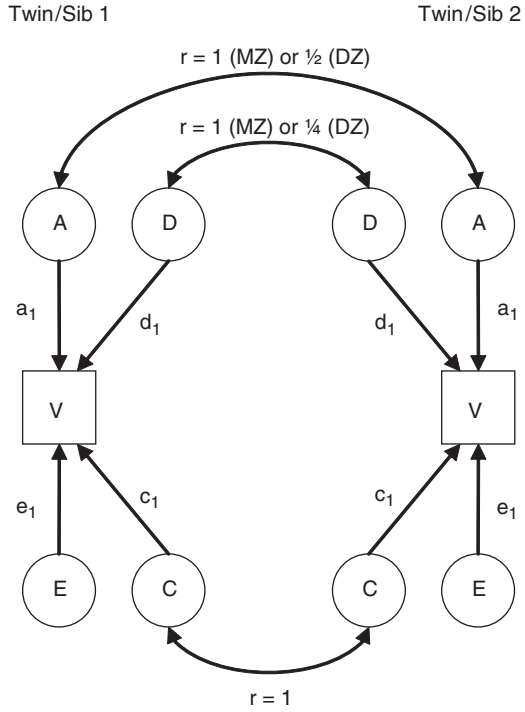

Figure 2. The univariate path model. The observed variables (V, assessed in two family members) are modeled as the weighted effects of unobserved variables (circles) representing additive genetic (A), dominant genetic (D), common environmental (C), and unique environmental (E) factors. Each of these factors has a unique pattern of correlation between MZ and DZ twins/siblings as indicated by the double headed arrows. The model presented here describes the relation between two family members, but can be extended to include all members. The genetic factor A is correlated $r = 1$ for MZ twin pairs and $r = 0.5$ for all other first-degree relatives; D is correlated 1 for MZ and $r = 0.25$ for other sibling pairs; C is correlated 1 between all MZ, DZ, and sibling pairs; E is uncorrelated ($r = 0$) between family members (no arrows). Note that in the extended twin design (with twins and siblings) the correlation matrix does not provide enough information to estimate D and C simultaneously: Either path coefficient d_1 or c_1 needs to constrained at 0.

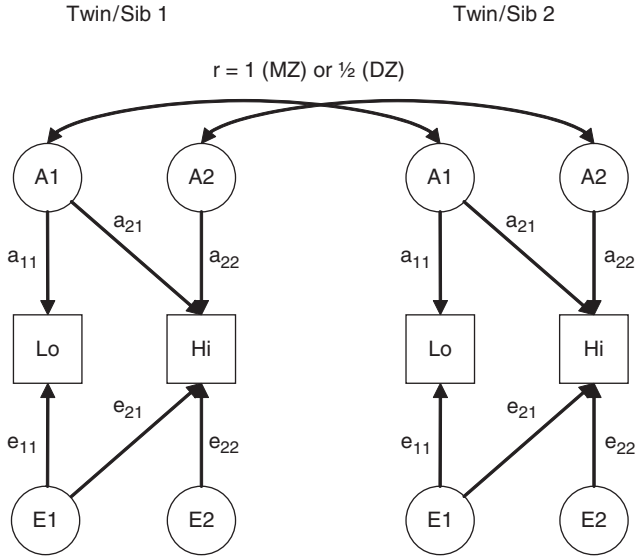

Figure 3. The bivariate path model explaining variance in the low and high memory load conditions. The model uses a Cholesky decomposition into additive genetic (A1, A2) and unique environmental factors (E1, E2). A1 reflects the expression of genes shared between the low and high load conditions. The model presented here describes the relation between two family members, but can be extended to include all members. Emergence of novel genes in the high load condition is represented by a_{22}.

is nonsignificant, the genetic correlation between the measures equals 1.

All genetic analyses were performed using Structural Equation Modeling implemented in the program Mx (Neale, Boker, Xie, and Maes, 2004). An extended twin design as used here provides data from families of variable size. Mx handles such unbalanced data sets via full information maximum likelihood, which uses the observed, raw data. To evaluate how well the specified model fits the observed data, the raw data option in Mx calculates the negative Log-Likelihood (LL) for each family following Lange, Westlake, and Spence (1976). Twice the difference between the likelihood of two nested models ($2\{LL_{full}$ model LL_{nested} model$\}$) is asymptotically distributed as χ^2. A high χ^2 against a low gain of degrees of freedom (Δdf) denotes a worse fit of the second, more restrictive model relative to the first model. By stepwise restricting the number of parameters, the most parsimonious model for the data set can be found. Each nested model is compared to the previous one. These nested comparisons can be applied to univariate models (e.g., comparing the fit of an AE model to the ADE model on a single lead in a single condition) or multivariate models (e.g., by equating heritabilities across sexes or experimental conditions). A linear regression model was employed to include effects of age cohort and sex on the observed scores. Additionally, a covariate was added to regress out a possible effect of equipment (Neuroscan or Poly, see above). For traits that showed a sex difference in variance, covariates were used to scale the variance of one group to equal that of the other group.

All effects were tested against an alpha level of .01. All alpha values between .05 and .01 were considered trends.

Results

Performance Data

Table 1 shows behavioral speed and accuracy scores in the low and high memory load conditions, separately for distractor and nondistractor trials. Response initiation time was barely affected by the difficulty level, but the accuracy data confirmed that the manipulation was effective. On average, the high memory load condition decreased spatial accuracy compared to the low memory load condition ($\chi^2 = 499.6$, $p < 10^{70}$). The added working memory load reduced the points earned by 3.5 units in the nondistractor condition and by 4.4 units in the distractor condition. The effect of the distractor itself interacted with memory load so that it reduced performance in the high but not in the low memory load condition ($\chi^2 = 71.6$, $p < 10^{-15}$). The effect size of the memory load manipulation (Cohen's $d = 3.31$) was much larger than that of the distractor effect (Cohen's $d = 0.86$). Therefore, and to increase signal-to-noise ratio, further analyses were collapsed across distractor and no-distractor trials.

SCP

Figure 4 shows the grand average ERP waves. Note that the early ERP components are visually compressed due to the long time

Table 1. *Effects of Memory Load and the Presence of Distractors on Response Speed and Spatial Accuracy*

	Low		High		Memory load effect (HighLow)		
	M	*SD*	*M*	*SD*	*M*	*SD*	Significance
Speed (ms)							
Distractor							
No	408	80.2	398	72.5	−9.4	37.8	***
Yes	395	71.9	397	67.7	1.5	28.2	n.s.
Accuracy (points earned)							
Distractor							
No	8.15	0.92	4.60	1.31	−3.55	1.40	***
Yes	8.09	0.95	3.70	1.32	−4.40	1.42	***

Note. Significance was tested with Structural Equation Modeling using Mx accounting for the within-family dependency of the data.
***$p < .0001$.

interval plotted. The ERP for channel Pz is expanded for illustration purposes. As can be seen, the warning stimulus that included an auditory beep produced a clear N1 that was maximal at Cz, consistent with many previous findings (e.g., Altenmüller & Gerloff, 1999). After that, two positive complexes developed related to the warning stimulus/fixation on event. Next, a small positive complex developed related to the target onset, which overlapped with the initial rise of the SCP. The SCP started to develop at around 400 ms after the warning stimulus and reached a maximum level about 1.7 s after trial onset. The large negativity following the imperative stimulus (ca. 5000–5500 ms) revealed in the more central locations is the Post-Imperative Negative Variation related to expectation to the feedback stimulus (Birbaumer et al., 1990)

Voltages during the SCP were significantly below baseline for all leads tested in both memory load conditions (Table 2, left panel). On most leads, the SCP appears to decay slowly, but this reflects in part the effect of the high-pass filtering. Largest SCPs were found along the midline. SCPs in the low and high memory load conditions were very similar in shape, but more negative voltages were found during the high memory load condition on all leads. The effects of memory load was largest for C3 and P3 and reached significance for F7, T7, C3, C4, P7, P3, Pz, P4, O1, and O2. The middle-aged adults showed significantly smaller SCPs at the midparietal leads in the high memory load condition (effects of age cohort at C4: 1.34, T8: 0.81, P3: 1.24, Pz: 1.85, P4: 1.84, and P8: 0.92) and more widespread in the low memory load condition (effect of age cohort at F1: 1.38, Fz: 1.60, F2: 1.27, F8: 1.26, C3: 1.25, Cz: 2.00, C4: 1.55, P3: 1.36, Pz: 2.02, P4: 1.75, P8: 0.88, T8: 1.12, O2: 1.01). No systematic effects of sex or Age × Sex interactions were found on the SCP.

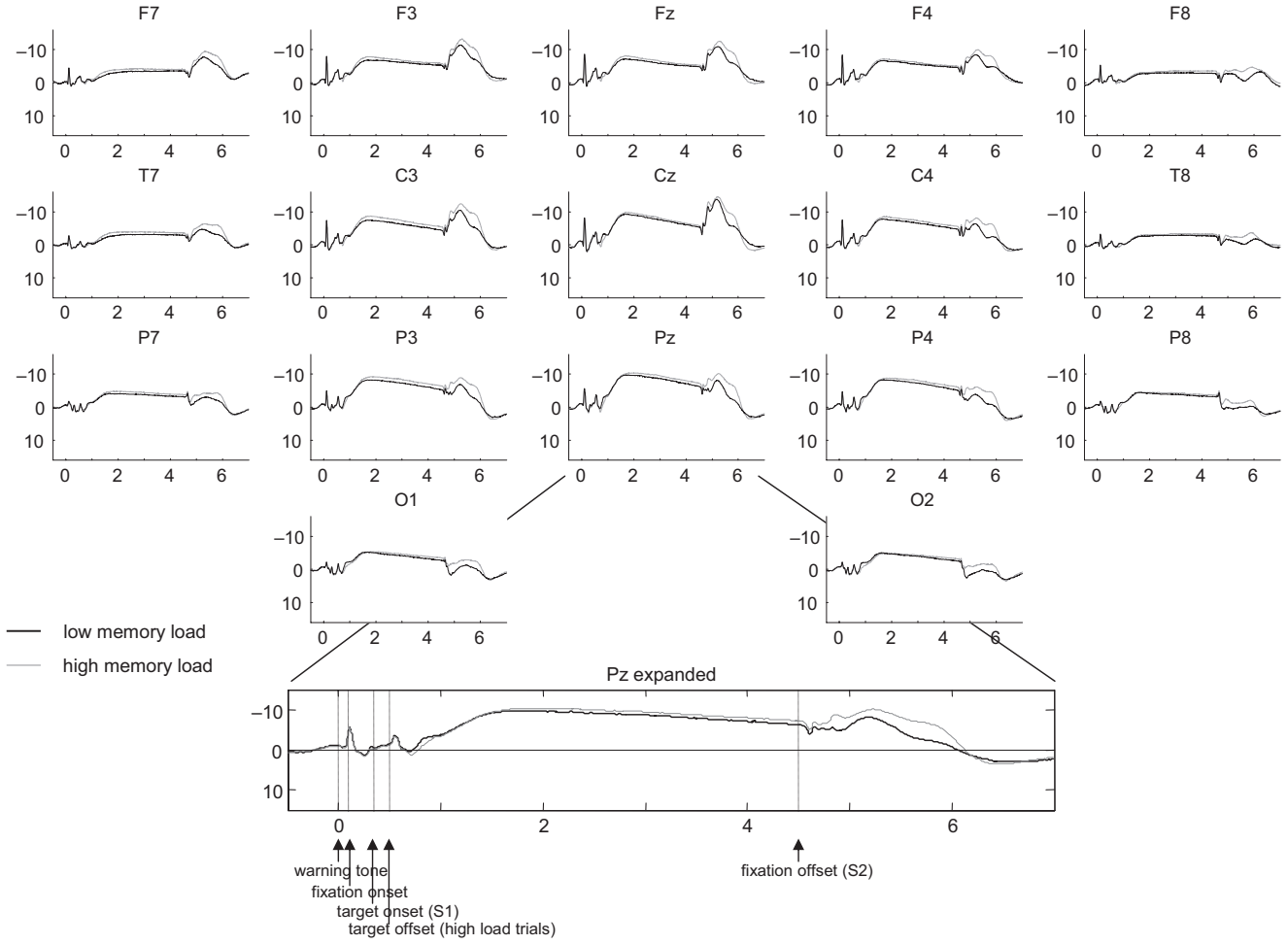

Figure 4. Grand average waveforms for the low and high memory load conditions. Negative is up.

Table 2. *Means of SCP, Upper Alpha Synchronization, and Theta Desynchronization in the Low and High Memory Load Conditions*

	SCP (μV)			Upper Alpha Synch. (dB)			Theta Desynch. (dB)		
Lead	Low	High	Memory load effect (high-low)	Low	High	Memory load effect (high-low)	Low	High	Memory load effect (high-low)
F7	−3.23	−4.03***	−0.80*	−0.04	0.01+	0.05	−0.92***	−0.79***	0.13***
F3	−5.76***	−6.34***	−0.58	0.05	0.10	0.05	−0.68***	−0.55***	0.13***
F1	−6.10***	−6.46***	−0.35	0.07	0.13	0.05*	−0.64***	−0.51***	0.13***
Fz	−5.67***	−6.33***	−0.65	0.07	0.13	0.06*	−0.63***	−0.50***	0.13***
F2	−5.52***	−6.21***	−0.68	0.07	0.12	0.05*	−0.65***	−0.52***	0.13***
F4	−5.30***	−5.77***	−0.47	0.04+	0.09	0.05*	−0.69***	−0.56***	0.13***
F8	−2.81***	−3.39***	−0.58	−0.05	0.00	0.05*	−0.91***	−0.82***	0.10***
T7	−3.02***	−3.69***	−0.67**	0.04	0.11*	0.07**	−0.58***	−0.48***	0.10***
C3	−5.97***	−7.06***	−1.08***	0.14*	0.18***	0.04	−0.64***	−0.53***	0.10***
Cz	−7.27***	−7.77***	−0.50	0.15**	0.22***	0.07***	−0.59***	−0.47***	0.11***
C4	−6.16***	−7.00***	−0.84**	0.16*	0.24***	0.08***	−0.67***	−0.56***	0.11***
T8	−2.70***	−3.08***	−0.38	0.11	0.18**	0.07*	−0.62***	−0.55***	0.07***
P7	−3.54***	−4.21***	−0.67**	0.23***	0.27***	0.05	−0.72***	−0.60***	0.11***
P3	−6.96***	−8.01***	−1.05***	0.28***	0.31***	0.04	−0.71***	−0.60***	0.11***
Pz	−8.20***	−9.07***	−0.87***	0.27***	0.33***	0.06	−0.66***	−0.55***	0.11***
P4	−6.86***	−7.63***	−0.77***	0.33***	0.40***	0.07*	−0.75***	−0.63***	0.12***
P8	−3.73***	−4.06***	−0.33	0.36***	0.42***	0.06	−0.79***	−0.67***	0.12***
O1	−3.96***	−4.49***	−0.54**	0.29***	0.29***	0.01	−1.03***	−0.92***	0.11***
O2	−3.66***	−4.07***	−0.41*	0.31***	0.32***	0.01	−1.05***	−0.92***	0.13***

$+p<.05$; $*p<.01$; $**p<.001$; $***p<.0001$.

Time-Frequency Analysis

Figures 5 and 6 show the results for the time-frequency analysis in the low and high memory load conditions averaged across all subjects. The plot colors are scaled in dB—that is, $10 \cdot \log_{10}(\mu V^2)$—compared to baseline power. There was a clear pattern of alpha and beta synchronization directly after stimulus presentation that corresponds to the ERP generation due to the warning tone and fixation onset (see oval A on the expanded lead figure). Slightly after target presentation, theta synchronization occurred (B) that is likely to reflect the late positive waves related to the target. Both A and B showed intertrial coherence (data not shown), indicating that the oscillatory activity is phase-locked to the stimulus event and will therefore also appear in the ERP. Within the delay interval between target and imperative stimulus, a clear theta desynchronization compared to baseline was seen (C). In addition, the same interval showed alpha synchronization on practically all leads and in both conditions in the delay interval (D). This upper alpha synchronization showed maximum power in both the 9.8-Hz and 10.8-Hz frequency bins. The weighted average frequency of these bins was 10.3 Hz. Because the average peak frequency for this sample is 9.9 Hz, the alpha synchronization could indeed be considered upper alpha synchronization. This finding is consistent with the previous finding of Bastiaansen et al. (2002), who used a subset of the current sample.

Like the SCP, upper alpha synchronization showed a distinct topographic pattern (Table 2, middle panel). Whereas frontal leads showed no significant change over baseline, all central and parietal and occipital leads did. Most leads showed a small sensitivity to memory load that reached significance for frontal leads (F1, Fz, F2, F4, and F8), the left and right temporal region (T7 and T8), the central region (Cz and C4), and the right parietal region (P4). Small sex differences emerged such that males had higher upper alpha synchronization than females (high memory load condition at F4: 0.15 dB; F8: 0.17 dB; T8: 0.15 dB; P4 and P8: 0.20 dB; low memory load condition F4: 0.16 dB, F8: 0.17 dB, P4: 0.18 dB). Upper alpha synchronization did not differ in the two age cohorts at any lead.

Significant theta desynchronization was found on all leads in both memory load conditions (Table 2, right panel) and was comparable across age cohort and sex. In contrast to the SCP and upper alpha synchronization, little topographic differentiation in the theta desynchronization was found. The effects of memory load were also significant across the entire scalp.

Heritability

No significant effects of shared environment (C) or dominant genetic effects (D) were found on any of the three ERP/EEG measures. Additive genetic effects were significant on all leads for alpha synchronization and theta desynchronization. For these measures, an AE model was significantly better than either an ADE or ACE model. For SCP, however, at those leads that showed a significant familial effect (the combined effect of A plus C), the effect of neither A or C alone reached significance. In all but two cases (O1 and Pz in the low memory load condition) the AE model provided the better fit. Therefore, and consistent with Hansell et al. (2001), we proceeded with an AE model for the SCP as we did for upper alpha synchronization and theta desynchronization. Table 3 shows the heritabilities derived from these models.

Heritability for the SCP in the low load condition did not reach significance on all leads, but a significant contribution of genetic factors was found in a right frontal leads (F4: 21% in the low load condition and 29% in the high load condition), left parietal-central leads (22%–36% in the low load condition and 30%–41% in the high load condition), and on left and right occipital leads (27% and 37% in the low load condition, 33% and 43% in the high load condition). Upper alpha synchronization was heritable across the entire scalp in both conditions (35%–60% in the low load condition and 35%–65% in the high load condition). Theta desynchronization also showed heritability across the scalp (18%–49% in the low load condition and 31%–50% in the high load condition.

Low versus High Memory Load

Inspection of Table 3 suggests that the pattern of heritability was similar in the low and high memory load conditions, but that

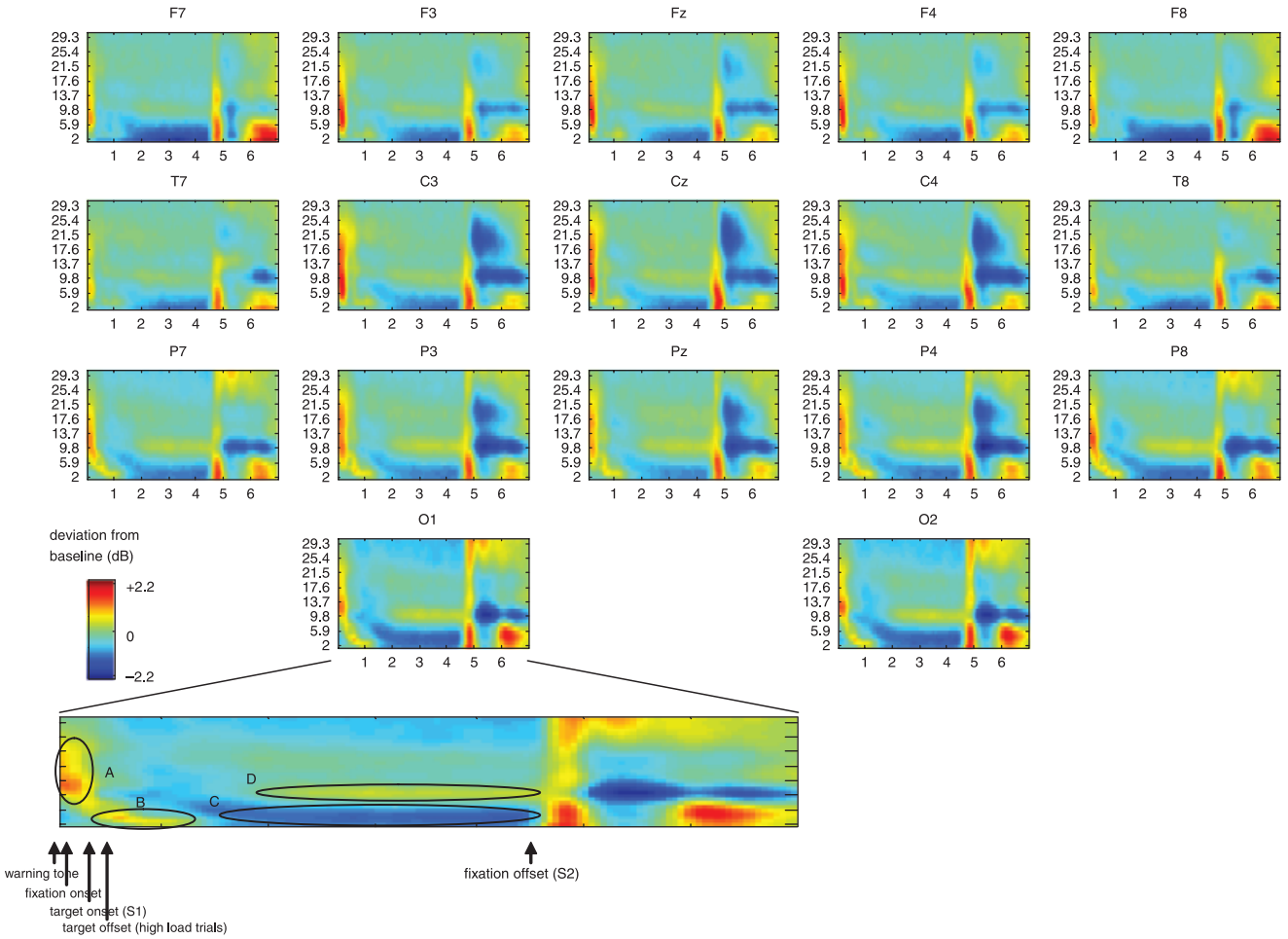

Figure 5. Grand average time-frequency plots for the low memory load condition. Time-frequency spectra were calculated using EEGLAB's *timef* function. Log transformed power relative to baseline was estimated from 2 Hz to 49.8 Hz in 50 frequencies 0.98 Hz apart. Hanning windowed sine/cosine wavelets were maximally 1024 ms wide and applied at 200 equally spaced time points from 12 ms to 6988 ms after the warning stimulus onset. Oval A shows activity induced by stimulus-locked sensory ERP activity. Oval B shows activity induced by stimulus-locked late ERP components. Oval C shows the response anticipation interval theta desynchronization. Oval D shows the upper alpha synchronization.

significant heritability estimates were often higher in the high load condition. Bivariate analyses showed that there was no evidence for a significant increase in heritability for the SCP and upper alpha synchronization on any of the leads. For theta desynchronization, however, increased heritability was found at F1 and Fz, and trends were found for F7, F3, F2, and T7. The decomposition into genetic and environmental variance revealed that the heritability increase for these leads was due to both an increase in genetic variance and a decrease in environmental variance, in about equal amounts.

Bivariate modeling across conditions revealed that the increase in genetic variance on these leads was not due to newly emerging genetic effects specific to the high memory load condition. That is, genes that were expressed during the high load condition were already expressed in the low load condition.

(Genetic) Correlations between the EEG/ERP Measures

Because the above results showed that the low and high memory load conditions yielded similar results in most cases but that—at least for theta desynchronization—the high memory load condition seemed genetically most informative, all cross-measure analyses were based on this condition. Table 4 shows the phenotypic correlation between the measures followed by the weighted genetic correlations. For instance, for lead P3 the phenotypic correlation between SCP and upper alpha synchronization was .20 with a genetic correlation of .19. As is clear from the table, the overlap between individual differences in SCP amplitude and upper alpha synchronization is very small and limited to Cz, C4, P7, P3, and Pz. A significant genetic contribution to these correlations could be established only for P3 and P4. Between SCP and theta desynchronization no significant correlation was found on any lead.

In contrast, upper alpha synchronization and theta desynchronization showed significant positive correlation across the entire scalp (r from .38 to .50). Many of the leads showed a significant genetic overlap and at least a trend toward significance. The weighted genetic correlations were on average 46% of the phenotypic correlation.

Discussion

Consistent with studies using the same or comparable delayed response or memory retention designs, the current data showed

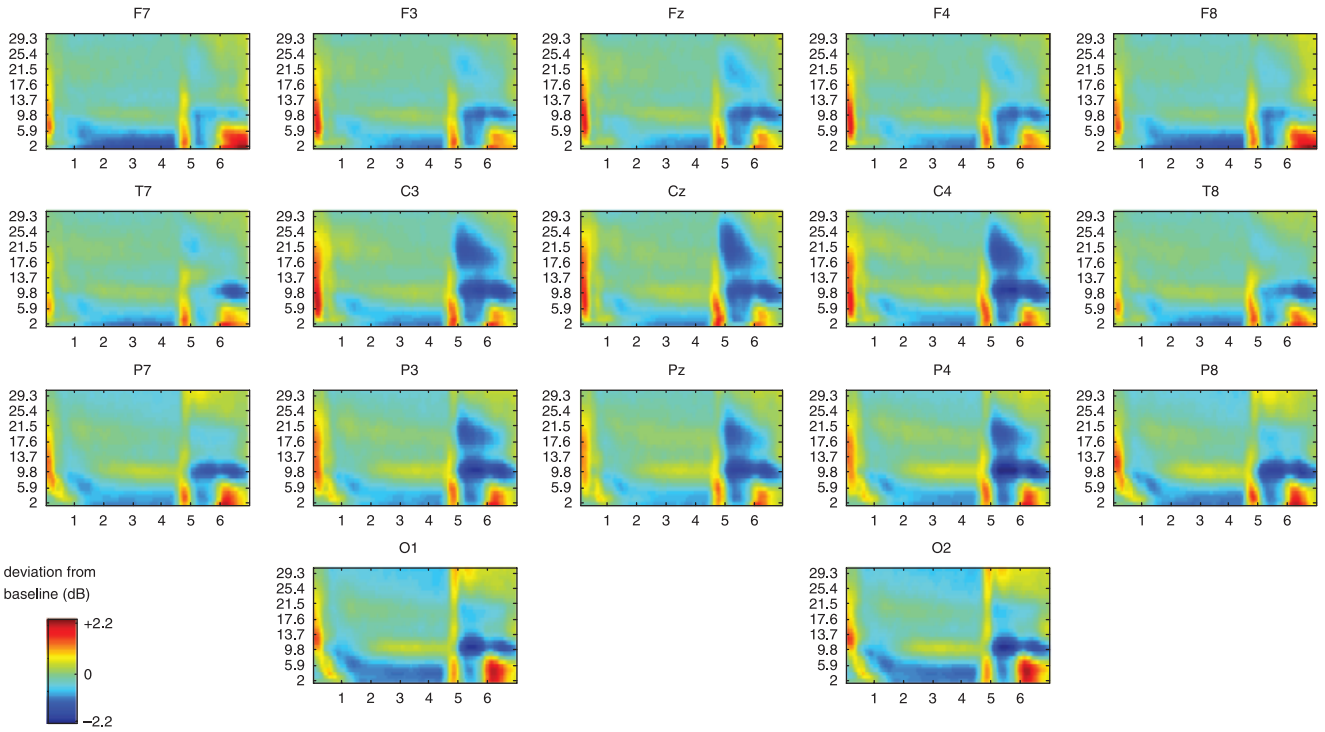

Figure 6. Grand average time-frequency plots for the high memory load conditions. For further specifications see Figure 5 legend.

not only a clear SCP, but also upper alpha synchronization in the response anticipation interval (SCP: e.g., Filipovic, Jahanshahi, & Rothwell, 2001; Hansell et al., 2001; alpha synchronization: e.g., Bastiaansen et al., 2002; Filipovic et al., 2001; Klimesch et al., 1999; Klimesch et al., 2007; Krause, Lang, Laine, Kuusisto, & Pörn, 1996). We also replicated the theta desynchonization in this interval previously observed in a subset of these subjects by Bastiaansen et al. (2002). In keeping with previous studies, we confirm that the amplitude of the SCP is modulated by working memory load (Cameron et al., 2003) and that the upper alpha synchronization and theta desynchronization seen during response anticipation also significantly increase with higher spatial working memory load.

Large individual differences were present in all three ERP/EEG measures, and we tested the relative contribution of genetic influences to these measures by comparing trait resemblance in siblings of varying degree of genetic relatedness (i.e., MZ and DZ twins and non-twin siblings). Significant heritability was found

Table 3. *Heritability Estimates from Univariate AE models of SCP, Upper Alpha Synchronization, and Theta Desynchronization for the Low and High Memory Load Conditions*

	SCP		Upper Alpha Synchronization		Theta Desynchronization	
Lead	Low	High	Low	High	Low	High
F7	7%	0%	40%***	43%***	19% +	32%***
F3	14%	16%	39%***	44%***	18% +	40%***
F1	17% +	21% +	37%***	43%***	21% +	45%***
Fz	22% +	25%*	41%***	48%***	28%*	50%***
F2	10%	12%	41%***	44%***	26%*	45%***
F4	21%*	29%**	40%***	42%***	25%*	39%***
F8	12%	19% +	39%***	45%***	23%*	34%***
T7	7%	4%	35%**	45%***	22%*	41%***
C3	26%*	30%**	41%***	35%***	29%**	41%***
Cz	19% +	30%**	39%***	38%***	34%***	48%***
C4	22%*	17% +	40%***	43%***	36%***	40%***
T8	7%	8%	35%**	50%***	22%*	38%***
P7	36%***	35%***	51%***	48%***	18% +	31%**
P3	34%***	41%***	51%***	45%***	31%**	37%***
Pz	29%**	35%***	52%***	53%***	45%***	46%***
P4	16% +	20% +	50%***	55%***	49%***	43%***
P8	19% +	15%	43%***	55%***	34%***	32%**
O1	37%***	43%***	60%***	64%***	44%***	35%***
O2	27%*	33%**	60%***	65%***	43%***	36%***

$+p<.05$; $*p<.01$; $**p<.001$; $***p<.0001$.

Table 4. *Phenotypic and Genetic Correlations between SCP, Upper Alpha Desynchronization, and Theta Synchronization in the High Memory Load Condition*

	SCP & Upper Alpha Sync.		SCP & Theta Desync.		Upper Alpha Sync. & Theta Desync.	
Lead	Phenotypic correlation	Weighted genetic correlation	Phenotypic correlation	Weighted genetic correlation	Phenotypic correlation	Weighted genetic correlation
F7	0.03	0.00	0.02	0.00	0.50***	0.17+
F3	0.03	−0.02	0.01	0.02	0.47***	0.22*
F1	0.04	0.01	−0.01	−0.02	0.54***	0.29*
Fz	0.06	−0.02	0.03	−0.03	0.41***	0.21*
F2	0.07	−0.02	0.03	−0.02	0.42***	0.20*
F4	0.09+	−0.03	0.03	−0.03	0.44***	0.19*
F8	0.04	0.01	0.05	0.07	0.46***	0.19*
T7	0.07	0.00	−0.01	0.00	0.49***	0.25***
C3	0.12+	0.10	−0.05	−0.04	0.49***	0.25**
Cz	0.13*	0.00	0.02	−0.02	0.39***	0.17+
C4	0.15*	0.14+	0.04	−0.01	0.42***	0.17+
T8	0.02	0.03	0.02	−0.01	0.47***	0.15+
P7	0.14*	0.10	0.01	0.01	0.45***	0.21*
P3	0.20**	0.19*	0.07	0.02	0.44***	0.18+
Pz	0.17*	0.15+	0.04	0.02	0.39***	0.15+
P4	0.14	0.19*	0.01	0.06	0.43***	0.25**
P8	0.07	0.04	0.00	0.03	0.44***	0.19*
O1	0.09	0.13+	−0.05	−0.04	0.43***	0.25**
O2	0.03	0.03	0.04	0.00	0.38***	0.21*

Note. No dominant genetic effects were found. The weighted genetic correlation was calculated as the additive genetic correlation r_A multiplied by the path loadings (see text).
+p < .05; *p < .01; **p < .001; ***p < .0001.

for SCP, upper alpha synchronization, and theta desynchronization. Focusing on significant effects in the high memory load condition, heritability varied from 25% to 43% for SCP. These estimates are comparable to those in earlier reports (Hansell et al., 2001, 2005), where heritabilities of 39% were found for the SCP in the high memory load condition in the same delayed response task. For upper alpha synchronization, heritability varied from 35% to 65%, and for theta desynchronization, heritability ranged from 31% to 50%. These estimates are lower than heritability of resting state oscillatory power in the same bands (Smit et al., 2005) but similar to other evoked responses such as the P300 and N1 (Anokhin, Heath, & Myers, 2004; Smit et al., 2007a, 2007b; van Beijsterveldt and van Baal, 2002). Note that genetic contribution to SCP was localized mainly in the right frontal, left parietal-central, and occipital areas, but for upper alpha synchronization and theta desynchronization, no clear topographic pattern in heritability could be distinguished.

Heritability was generally higher in the high memory load condition than in the low memory load condition. For theta desynchronization some evidence for an increase of heritability was found in the frontal areas, which reached significance at leads Fz and F1. For other leads, however, and for SCP and upper alpha synchronization, we must conclude that the memory load manipulation did not do much to reduce unique environmental variance (including noise) or increase genetic variance. In addition, there was no evidence for the emergence of genetic variance specific to the high memory load condition, indicating that individual differences in both conditions are driven by the same set of genes.

From the literature, the antecedent conditions evoking the SCP seem to be threefold: cued expectancy of a salient stimulus, an actual motor response, and motivational salience of the response. That is, the SCP only develops after a cue or warning stimulus, and it is strongly reduced in amplitude when no overt response is required. A stronger negative potential is obtained when a feedback stimulus is an aversive tone or a shock (Rockstroh et al., 1989). The interpretation of the SCP has been manifold (Birbaumer et al., 1990) but most sources consider it to reflect active inhibition of some areas and facilitation of others. This was already defined in 1976 by Deecke et al. (Deecke, 1976, cited by Rockstroh et al., 1989, p. 168) as ''a general facilitation process, preactivating those brain regions which will be needed under the special experimental condition.'' A modern definition restates this as ''the allocation of attentional resources for action'' (Filipovic et al., 2001; Rockstroh et al., 1989) or ''attentive effort'' (Brunia & van Boxtel, 2001).

The interpretation of alpha oscillations has witnessed changes in recent years. From some of the earliest human scalp recorded EEG investigations, it had been proposed that alpha oscillations desynchronize upon activation of the cortical area under scrutiny (Adrian & Mathews, 1934). Therefore, alpha rhythms (and related rhythms such as mu) were thought to appear only in states of inactivity, that is, during cortical ''idling.'' Increasingly, however, alpha synchronization has been ascribed a more active role as an index of top-down inhibition (Başar, Schurmann, Basar-Eroglu, & Karakas, 1997; Hummel, Andres, Altenmuller, Dichgans, & Gerloff, 2002; Jensen et al., 2002; Joskisch & Jensen, 2007; Klimesch, Doppelmayr, & Hanslmayr, 2006; Klimesch et al., 2007; Neuper, Wortz, & Pfurtscheller, 2006; Sauseng et al., 2005) or alertness (Knyazev, Savostyanov, & Levin, 2006), rather than as a measure of ''cortical idling.''

In the introduction we suggested that the SCP and alpha activity share antecedent conditions and that therefore they may perhaps be closely related neural phenomena. This idea is reinforced by the potential sharing of thalamo-cortical loops as the most likely source of slow cortical potentials such as the SCP as well as alpha generation (Birbaumer et al., 1990; Danos et al., 2001; Goldman et al., 2002; Nagai et al., 2004; Rockstroh et al., 1989; Schreckenberger et al., 2004). Alternatively, the reticular

formation (RF) may be the primary source, as the RF is known to modulate thalamic activity (the reticular formation of the thalamus) and to affect both slow cortical potentials and oscillatory activity (Birbaumer et al., 1990; Rockstroh et al., 1989). It is even possible that the SCP is, in part, directly generated by a change in alpha synchronization (Klimesch et al., 2007; Min et al., 2007; Nikulin et al., 2007; Sauseng et al., 2005). On the basis of the idea that SCP and alpha power may share a neural substrate, we hypothesized that individual differences in both measures would be correlated and influenced by a common set of genes (see also Schmitt et al., 2008). The multivariate analysis presented here only provided partial support for this hypothesis, as SCP and upper alpha synchronization were (genetically) uncorrelated for most leads, although a significant correlation was found for alpha synchronization and SCP on the right central and left parietal scalp areas.

Some previous studies, using a comparable design, had already alluded to this outcome, although they did so on the basis of very small sample sizes. For example, Filipovic et al. (2001) used a go/no-go task that evoked a small alpha synchronization in a 3-s interval between a cue and imperative stimulus. Observing no condition effect for alpha synchronization whereas SCP showed a clear go/no-go difference, they concluded that alpha synchronization and SCP reflected different aspects of cognitive processing. Pfurtscheller and Aranibar (1977) reached the same conclusion on the basis of different scalp distribution for alpha synchronization (sensory areas) and SCP (motor areas). Fan et al. (2007) also reported no correlation between alpha activity of several dipoles with the SCP in a 2.5-s interval between a cue and imperative stimulus. Taken together, the bulk of the evidence suggests that the SCP and alpha synchronization reflect unique aspects of response anticipation. In keeping with this, the individual differences in these measures may index different genetic aspects of response anticipation: Upper alpha synchronization may reflect genetic aspects of overall arousal, whereas the SCP may index genetic effects on the task-specific visuo-spatio-motor aspects of the delayed response task.

SCP and alpha synchronization were accompanied by a significant theta desynchronization throughout the interval between warning stimulus and response stimulus. On top of this overall decrease in theta power, an increase in working memory load caused a relative increase of theta power. This is consistent with previous studies reporting theta synchronization during episodic memory processing (e.g., Gevins, Smith, McEvoy, & Yu, 1997; Klimesch, 1999), a two-back task (Krause et al., 2000), and a spatial memory task (Jensen & Tesche, 2002). In keeping with Bastiaansen et al. (2002) we interpret the theta desynchronization to have a functional role in enhancing the signal-to-noise ratio of the activity in the hippocampal-cortical loops. We do not, however, replicate the previously reported topography. Instead, theta desynchronization was found across the entire scalp, as was the memory-induced attenuation of this effect. During both memory load conditions, individual differences in theta desynchronization showed consistent overlap with differences in upper alpha synchronization (r from about .40 to .50), and about 50% of this correlation was due to shared genes. This (genetic) correlation between alpha synchronization and theta desynchronization is a novel finding. Taking the substantial heritability of both, it suggests that the alpha and theta responses to this type of task reflects a stable bivariate characteristic of individuals that could be a useful endophenotype in genetic research of brain function.

Some limitations of this study should be noted. The basic approach in this study is a hybrid of the universal processes and an individual differences design. In the universal processes approach we assume that the same antecedent conditions will produce an SCP, upper alpha synchronization, and theta desynchronization in all subjects. But to test whether these EEG/ERP phenomena derive from the same neural substrate we used an individual differences approach. This means that we tested whether the amplitude of the SCP and the extent of upper alpha synchronization and theta desynchronization were correlated across individuals. This, as has been shown above, did not appear to be the case. However, one may argue that within a single individual, these measures might still be correlated. To test this, a parametric approach would be needed that manipulates the amplitude of the SCP in a within-subject repeated measures. This could be done by using multiple memory loads as well as multiple levels of motivational salience of the task by adding larger incentives like threat of shock or tones on errors. Here, we used only two task conditions (low and high memory load), which did not allow computation of within-subject correlations of SCP, alpha synchronization, and theta desynchronization. It is hard to envision how the SCP could correlate with upper alpha synchronization and theta desynchronization within each subject and yet show no correlation at the between-subjects level. Still, this possibility cannot be ruled by the current design.

To summarize, response anticipation evokes an SCP together with significant upper alpha synchronization and theta desynchronization. Each of these traits showed significant heritability, classifying them as viable endophenotypes for genetic research on basic brain functions. Genetic effects on the SCP are specific to this measure, whereas alpha synchronization and theta desynchronization have about half of their segregating genes in common, suggesting some biological common ground. In the average subject, increasing working memory load induced marked changes in all three measures. These changes, however, are not heritable and therefore not viable as genetic markers of interindividual variability.

REFERENCES

Adrian, E. D., & Mathews, B. H. (1934). The Berger rhythm: Potential changes from the occipital lobes in man. *Brain and Cognition*, *57*, 355–385.

Altenmüller, E. O., & Gerloff, C. (1999). Psychophysiology and the EEG. In E. Niedermeyer & F. Lopes da Silva (Eds.), *Electroencephalography* (4th ed.). Philadelphia: Lippincott Williams & Wilkins.

Anokhin, A. P., Heath, A. C., & Myers, E. (2004). Genetics, prefrontal cortex, and cognitive control: A twin study of event-related brain potentials in a response inhibition task. *Neuroscience Letters*, *368*, 314–318.

Başar, E., Schurmann, M., Basar-Eroglu, C., & Karakas, S. (1997). Alpha oscillations in brain functioning: An integrative theory. *International Journal of Psychophysiology*, *26*, 5–29.

Basile, L. F., Anghinah, R., Ribeiro, P., Ramos, R. T., Piedade, R., Ballester, G., et al. (2007). Interindividual variability in EEG correlates of attention and limits of functional mapping. *International Journal of Psychophysiology*, *65*, 238–251.

Bastiaansen, M., & Hagoort, P. (2003). Event-induced theta responses as a window on the dynamics of memory. *Cortex*, *39*, 967–992.

Bastiaansen, M. C., Posthuma, D., Groot, P. F., & de Geus, E. J. (2002). Event-related alpha and theta responses in a visuo-spatial working memory task. *Clinical Neurophysiology*, *113*, 1882–1893.

Birbaumer, N., Elbert, T., Canavan, A. G., & Rockstroh, B. (1990). Slow potentials of the cerebral cortex and behavior. *Physiological Reviews*, *70*, 1–41.

Boomsma, D., Busjahn, A., & Peltonen, L. (2002). Classical twin studies and beyond. *Nature Reviews. Genetics*, *3*, 872–882.

Boomsma, D. I., Vink, J. M., van Beijsterveldt, T. C., de Geus, E. J., Beem, A. L., Mulder, E. J., et al. (2002). Netherlands Twin Register: A focus on longitudinal research. *Twin Research*, *5*, 401–406.

Brunia, C. H., & van Boxtel, G. J. (2001). Wait and see. *International Journal of Psychophysiology*, *43*, 59–75.

Cameron, A. M., Geffen, G. M., Kavanagh, D. J., Wright, M. J., McGrath, J. J., & Geffen, L. B. (2003). Event-related potential correlates of impaired visuospatial working memory in schizophrenia. *Psychophysiology*, *40*, 702–715.

Danos, P., Guich, S., Abel, L., & Buchsbaum, M. S. (2001). EEG alpha rhythm and glucose metabolic rate in the thalamus in schizophrenia. *Neuropsychobiology*, *43*, 265–272.

De Geus, E. J., Kupper, N., Boomsma, D. I., & Snieder, H. (2007). Bivariate genetic modeling of cardiovascular stress reactivity: Does stress uncover genetic variance? *Psychosomatic Medicine*, *69*, 356–364.

Delorme, A., & Makeig, S. (2004). EEGLAB: An open source toolbox for analysis of single-trial EEG dynamics including independent component analysis. *Journal of Neuroscience Methods*, *134*, 9–21.

Doppelmayr, M., Klimesch, W., Hodlmoser, K., Sauseng, P., & Gruber, W. (2005). Intelligence related upper alpha desynchronization in a semantic memory task. *Brain Research Bulletin*, *66*, 171–177.

Doppelmayr, M., Klimesch, W., Sauseng, P., Hodlmoser, K., Stadler, W., & Hanslmayr, S. (2005). Intelligence related differences in EEG-bandpower. *Neuroscience Letters*, *381*, 309–313.

Fan, J., Kolster, R., Ghajar, J., Suh, M., Knight, R. T., Sarkar, R., et al. (2007). Response anticipation and response conflict: An event-related potential and functional magnetic resonance imaging study. *Journal of Neuroscience*, *27*, 2272–2282.

Filipovic, S. R., Jahanshahi, M., & Rothwell, J. C. (2001). Uncoupling of contingent negative variation and alpha band event-related desynchronization in a go/no-go task. *Clinical Neurophysiology*, *112*, 1307–1315.

Gevins, A., Smith, M. E., McEvoy, L., & Yu, D. (1997). High-resolution EEG mapping of cortical activation related to working memory: Effects of task difficulty, type of processing, and practice. *Cerebral Cortex*, *7*, 374–385.

Goldman, R. I., Stern, J. M., Engel, J. Jr., & Cohen, M. S. (2002). Simultaneous EEG and fMRI of the alpha rhythm. *NeuroReport*, *13*, 2487–2492.

Hansell, N. K., Wright, M. J., Geffen, G. M., Geffen, L. B., Smith, G. A., & Martin, N. G. (2001). Genetic influence on ERP slow wave measures of working memory. *Behavior Genetics*, *31*, 603–614.

Hansell, N. K., Wright, M. J., Luciano, M., Geffen, G. M., Geffen, L. B., & Martin, N. G. (2005). Genetic covariation between event-related potential (ERP) and behavioral non-ERP measures of working-memory, processing speed, and IQ. *Behavior Genetics*, *35*, 695–706.

Hummel, F., Andres, F., Altenmuller, E., Dichgans, J., & Gerloff, C. (2002). Inhibitory control of acquired motor programmes in the human brain. *Brain*, *125*, 404–420.

Jausovec, N., & Jausovec, K. (2004). Differences in induced brain activity during the performance of learning and working-memory tasks related to intelligence. *Brain and Cognition*, *54*, 65–74.

Jensen, O., Gelfand, J., Kounios, J., & Lisman, J. E. (2002). Oscillations in the alpha band (9–12 Hz) increase with memory load during retention in a short-term memory task. *Cerebral Cortex*, *12*, 877–882.

Jensen, O., & Tesche, C. D. (2002). Frontal theta activity in humans increases with memory load in a working memory task. *European Journal of Neuroscience*, *15*, 1395–1399.

Jokisch, D., & Jensen, O. (2007). Modulations of gamma and alpha activity during a working memory task engaging the dorsal and ventral stream. *Journal of Neuroscience*, *27*, 3244–3251.

Klimesch, W. (1999). EEG alpha and theta oscillations reflect cognitive and memory performance: A review and analysis. *Brain Research: Brain Research Reviews*, *29*, 169–195.

Klimesch, W., Doppelmayr, M., & Hanslmayr, S. (2006). Upper alpha ERD and absolute power: Their meaning for memory performance. *Progress in Brain Research*, *159*, 151–165.

Klimesch, W., Doppelmayr, M., Schwaiger, J., Auinger, P., & Winkler, T. (1999). ''Paradoxical'' alpha synchronization in a memory task. *Brain Research. Cognitive Brain Research*, *7*, 493–501.

Klimesch, W., Sauseng, P., & Hanslmayr, S. (2007). EEG alpha oscillations: The inhibition-timing hypothesis. *Brain Research Reviews*, *53*, 63–88.

Knyazev, G. G., Savostyanov, A. N., & Levin, E. A. (2006). Alpha synchronization and anxiety: Implications for inhibition vs. alertness hypotheses. *International Journal of Psychophysiology*, *59*, 151–158.

Krause, C. M., Lang, A. H., Laine, M., Kuusisto, M., & Pörn, B. (1996). Event-related EEG desynchronization and synchronization during an auditory memory task. *Electroencephalography and Clinical Neurophysiology*, *98*, 319–326.

Krause, C. M., Sillanmaki, L., Koivisto, M., Saarela, C., Haggqvist, A., Laine, M., et al. (2000). The effects of memory load on event-related EEG desynchronization and synchronization. *Clinical Neurophysiology*, *111*, 2071–2078.

Lange, K., Westlake, J., & Spence, M. A. (1976). Extensions to pedigree analysis. III. Variance components by the scoring method.. *Annals of Human Genetics*, *39*, 485–491.

Makeig, S. (1993). Auditory event-related dynamics of the EEG spectrum and effects of exposure to tones. *Electroencephalograaphy and Clinical Neurophysiology*, *86*, 283–293.

Makeig, S., Jung, T. P., Bell, A. J., Ghahremani, D., & Sejnowski, T. J. (1997). Blind separation of auditory event-related brain responses into independent components. *Proceedings of the National Academy of Sciences, USA*, *94*, 10979–10984.

Min, B. K., Busch, N. A., Debener, S., Kranczioch, C., Hanslmayr, S., Engel, A. K., et al. (2007). The best of both worlds: Phase-reset of human EEG alpha activity and additive power contribute to ERP generation. *International Journal of Psychophysiology*, *65*, 58–68.

Nagai, Y., Critchley, H. D., Featherstone, E., Fenwick, P. B., Trimble, M. R., & Dolan, R. J. (2004). Brain activity relating to the contingent negative variation: An fMRI investigation. *NeuroImage*, *21*, 1232–1241.

Neale, M. C., Boker, S. M., Xie, G., & Maes, H. H. (2004). *Mx: Statistical Modeling* (6th ed.). Richmond, VA: Virginia Commonwealth University.

Neuper, C., Wortz, M., & Pfurtscheller, G. (2006). ERD/ERS patterns reflecting sensorimotor activation and deactivation. *Progress in Brain Research*, *159*, 211–222.

Nikulin, V. V., Linkenkaer-Hansen, K., Nolte, G., Lemm, S., Muller, K. R., Ilmoniemi, R. J., et al. (2007). A novel mechanism for evoked responses in the human brain. *European Journal of Neuroscience*, *25*, 3146–3154.

Perez-Edgar, K., Fox, N. A., Cohn, J. F., & Kovacs, M. (2006). Behavioral and electrophysiological markers of selective attention in children of parents with a history of depression. *Biological Psychiatry*, *60*, 1131–1138.

Pfurtscheller, G., & Aranibar, A. (1977). Event-related cortical desynchronization detected by power measurements of scalp EEG. *Electroencephalography and Clinical Neurophysiology*, *42*, 817–826.

Posthuma, D., Beem, A. L., de Geus, E. J., Van Baal, G. C., von Hjelmborg, J. B., Iachine, I., et al. (2003). Theory and practice in quantitative genetics. *Twin Research*, *6*, 361–376.

Posthuma, D., Neale, M. C., Boomsma, D. I., & de Geus, E. J. (2001). Are smarter brains running faster? Heritability of alpha peak frequency, IQ, and their interrelation. *Behavior Genetics*, *31*, 567–579.

Rockstroh, B., Elbert, T., Canavan, A., Lutzenberger, W., & Birbaumer, N. (1989). *Slow cortical potentials and behavior* (2nd ed.). M ü nchen: Urban & Schwarzenberg.

Ruchkin, D. S., Canoune, H. L., Johnson, R. Jr., & Ritter, W. (1995). Working memory and preparation elicit different patterns of slow wave event-related brain potentials. *Psychophysiology*, *32*, 399–410.

Sauseng, P., Klimesch, W., Schabus, M., & Doppelmayr, M. (2005). Fronto-parietal EEG coherence in theta and upper alpha reflect central executive functions of working memory. *International Journal of Psychophysiology*, *57*, 97–103.

Schmitt, J. E., Lenroot, R. K., Wallace, G. L., Ordaz, S., Taylor, K. N., Kabani, N., et al. (2008). Identification of genetically mediated

cortical networks: A multivariate study of pediatric twins and siblings. *Cerebral Cortex*, *18*, 1737–1747.

Schreckenberger, M., Lange-Asschenfeldt, C., Lochmann, M., Mann, K., Siessmeier, T., Buchholz, H. G., et al. (2004). The thalamus as the generator and modulator of EEG alpha rhythm: A combined PET/EEG study with lorazepam challenge in humans. *NeuroImage*, *22*, 637–644.

Smit, D. J., Posthuma, D., Boomsma, D. I., & de Geus, E. J. (2005). Heritability of background EEG across the power spectrum. *Psychophysiology*, *42*, 691–697.

Smit, D. J., Posthuma, D., Boomsma, D. I., & de Geus, E. J. (2007a). Heritability of anterior and posterior visual N1. *International Journal of Psychophysiology*, *66*, 196–204.

Smit, D. J., Posthuma, D., Boomsma, D. I., & de Geus, E. J. (2007b). Genetic contribution to the P3 in young and middle-aged adults. *Twin Research and Human Genetics*, *10*, 335–347.

Smit, D. J., Stam, C. J., Posthuma, D., Boomsma, D. I., & de Geus, E. J. (2008). Heritability of ''small-world'' networks in the brain: A graph theoretical analysis of resting-state EEG functional connectivity. *Human Brain Mapping*, *29*, 1368–1378.

Steriade, M. (2000). Corticothalamic resonance, states of vigilance and mentation. *Neuroscience*, *101*, 243–276.

Strehl, U., Trevorrow, T., Veit, R., Hinterberger, T., Kotchoubey, B., Erb, M., et al. (2006). Deactivation of brain areas during self-regulation of slow cortical potentials in seizure patients. *Applied Psychophysiology and Biofeedback*, *31*, 85–94.

van Beijsterveldt, C. E., & van Baal, G. C. (2002). Twin and family studies of the human electroencephalogram: A review and a meta-analysis. *Biological Psychology*, *61*, 111–138.

Walter, W. G. (1964). Slow potential waves in the human brain associated with expectancy, attention and decision. *Archiv Psychiatrie und Nervenkrankheiten*, *206*, 309–322.

Walter, W. G., Cooper, R., Aldridge, V. J., McCallum, W. C., & Winter, A. L. (1964). Contingent negative variation: An electric sign of sensorimotor association and expectancy in the human brain. *Nature*, *203*, 380–384.

(Received February 13, 2008; Accepted May 8, 2008)